SUPERCONDUCTING LINAC FOR THE RARE ISOTOPE SCIENCE PROJECT

H. J. Kim, H. J. Cha, M. O. Hyun, H. J. Jang, H. C. Jung,
Y. K. Kim, M. K. Lee, G.-T. Park, Institute for Basic Science, Daejeon, Korea

Abstract

The RISP (Rare Isotope Science Project) has been proposed as a multi-purpose accelerator facility for providing beams of exotic rare isotopes of various energies. It can deliver ions from proton to Uranium. Proton and Uranium beams are accelerated upto 600 MeV and 200 MeV/u respectively. The facility consists of three superconducting linacs of which superconducting cavities are independently phased. Requirement of the linac design is especially high for acceleration of multiple charge beams. In this paper, we present the RISP linac design, the prototyping of superconducting cavity and cryomodule.

INTRODUCTION

The Rare Isotope Science Project accelerator has been planned to study heavy ion of nuclear, material and medical science at the Institute for Basic Science. It can deliver ions from proton to Uranium with a final beam energy, for an example, 200 MeV/u for Uranium and 600 MeV for proton, and with a beam current range from 8.3 pμA (Uranium) to 660 pμA (proton) [1,2]. The facility consists of three superconducting linacs of which superconducting cavities are independently phased and operating at three different frequencies, namely 81.25, 162.5 and 325 MHz.

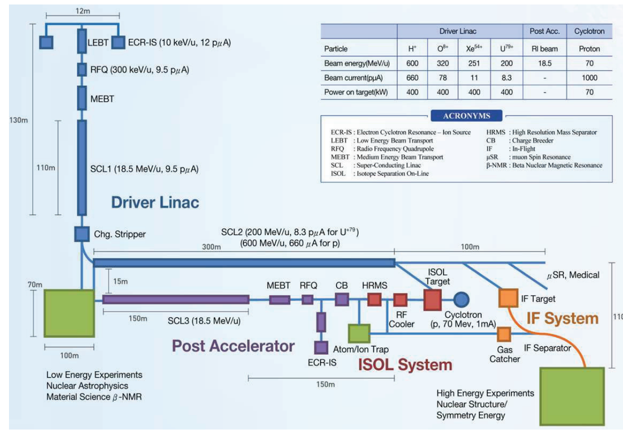

Figure 1: Layout of the RISP accelerator.

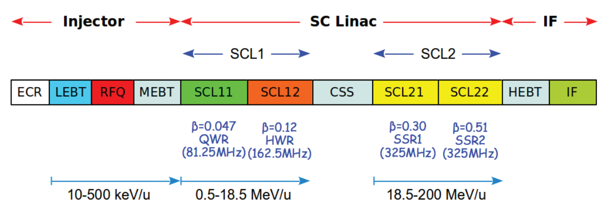

Figure 2: The RAON linear accelerator.

SUPERCONDUCTING LINAC

Lattice Design

The configuration of the accelerator facility within the rare isotope science project is shown in Fig. 1. An injector system accelerates a heavy ion beam to 500 keV/u and creates the desired bunch structure for injection into the superconducting linac. The injector system comprises an electron cyclotron resonance ion source, a low energy beam transport, a radio frequency quadrupole, and a medium energy beam transport. The superconducting driver linac accelerates the beam to 200 MeV/u. The driver linac is divided into three different sections as shown in Fig. 2: low energy superconducting linac (SCL1), charge stripper section (CSS) and high energy superconducting linac (SCL2). The SCL1 accelerates beam to 18.5 MeV/u. The SCL1 uses the two different families of superconducting resonators, i.e., quarter wave resonator (QWR) and half wave resonator (HWR). The CSS accepts beam at 18.5 MeV/u. The charge stripper strips electrons from heavy ion beams to enhance the acceleration efficiency in the high energy linac section. The SCL2 accepts beam at 18.5 MeV/u and accelerates it to 200 MeV/u. The SCL2 uses the two types of single spoke resonators, i.e., SSR1 and SSR2. The SCL2 provides beam into the in-flight fragmentation (IF) system via a high energy beam transport (HEBT). The post accelerator (SCL3) is designed to accelerate the rare isotopes produced in the ISOL (Isotope Separation On-Line) system. The SCL3 is, in principle, a duplicate of the driver linac up to low energy linear accelerator. The accelerated rare isotope beams are reaccelerated in the SCL2. Hence, the RISP accelerator provides a large number of rare isotopes with high intensity and with various beam energies [3].

For the actual SCL, machine imperfections cannot be avoided. The error comes from the misalignment of the linac elements and the limitation of manufacturing accuracy and various control errors. For instance, steering magnets are used to correct beam orbit displacements. In the baseline design of the RISP linac, steering magnets are placed where normal conducting quadrupoles are. The misalignment analysis includes all superconducting cavities and focusing elements assuming a uniform distribution. Table 1 summarizes tolerances for the lattice consisting of superconducting cavity and normal conducting quadrupole. In the misalignment and RF error analysis, charge states of 33+ and 34+ of Uranium beams are used. Effect of machine imperfection on beam envelope is shown in Fig. 3. The maximum envelope is kept well below the transverse aperture 20

ISBN 978-3-95450-142-7

Table 1: Machine Imperfection of RISP Lattice

Parameters	SC Cavity	Quadrupole
Displacement (mm)	±1	±0.15
Phase (deg)	±1	-
Amplitude (%)	±1	-
Rotation (mrad)	±5	±5

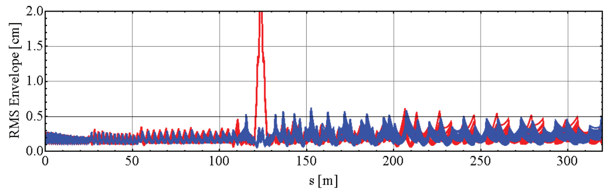

Figure 3: Plot of rms and maximum horizontal envelope for the driver linac due to machine imperfections.

mm in the low energy linac. The envelope is under 25 mm in the high energy linac.

Superconducting Cavity

In the optimization of superconducting cavity, the fabrication cost, symmetry of transversal field around drift tubes, and minimization of peak fields are mainly concerned. The detuning due to the tolerances of fabrication and the frequency sensitivities to mechanical deforming are estimated. The cavity is fabricated by electron beam welding of hydroformed 3 mm Niobium sheets, drift tube and 4 additional ports without bottom flange. Two ports in the lower end are added for RF power and pickup coupling. The other two ports are installed for evacuation and high pressure rinsing. The prototype of QWR has been fabricated by RRR 300 Niobium as shown in Fig. 4. The normal operating frequency of QWR at a cryogenic temperature is 81.25 MHz, but the traget frequency before a final welding is set to be 80.85 Mhz through the simulation of frequency changes due to external pressures, cooling-down to cryogenic temperature, BCP, welding shrinkage as shown in Table 2. Figure 5 shows the prototype of half wave resonator. Both QWR and HWR prototypes are under vertical test.

Single spoke resonator design has been upgraded [4]. The previous design of SSR was based on end-walls with flat areas. In a recent design, the end-walls are changed

Figure 4: Prototype of quarter wave resonator.

Table 2: Frequency Shift due to Various Sources

Frequency shift	QWR[MHz]	HWR[MHz]
Resonant frequency	81.25	162.5
External pressure (130 kPa)	81.27	162.55
Cool down (293 K → 4 K)	81.27	162.55
Vaccum	81.068	162.19
BCP (150 μm)	81.069	162.19
Welding shrikage (0.6 mm)	80.898	162.12
Clamp-up test	80.855	162.10

Figure 5: Prototype of half wave resonator.

from flat to round shape. We have performed simulations on electromagnetic analysis with changing the design parameters of the single spoke resonator. Figure 6 shows the prototype of SSR1 and SSR2. Table 3 summarizes the parameters of four different superconducting cavities for the RISP superconducting linac. Prototype of RF coupler has been fabricated and tested, shown in Fig. 7. Figure 8 shows conceptual design of slow tuner for QWR [5]. Blue arrow means the beam direction, and black structure is slow tuner. Right side of slow tuner is worm-worm wheel components which reduce speed and increase force. From cavity and liquid helium jacket design, cavity's beam port flange is connected with jacket body so that pulling or pushing beam port flange is most effective for tuning cavity.

Cryomodule

The linac has five types of cryomodules for four different kinds of cavities [6]. The main roles of the cryomodules are maintaining operating condition of superconducting cavities and alignment of the cavities along the beam

Figure 6: Prototyping of single spoke resonators: SSR1 (left) and SSR2 (right).

Table 3: Superconducting Cavity Parameters

Parameter	Unit	QWR	HWR	SSR1	SSR2
Frequency	MHz	81.25	162.5	325	325
β_g		0.047	0.12	0.30	0.51
$L_{eff} = \beta_g \lambda$	m	0.173	0.221	0.277	0.452
Q	10^9	2.1	4.1	9.2	10.5
QR_s	Ω	21	42	98	112
R/Q	Ω	468	310	246	296
E_{acc}	MV/m	5.2	5.9	6.9	8.6
E_{peak}/E_{acc}		5.6	5.0	6.3	7.2
B_{peak}/E_{acc}	mT/(MV/m)	9.3	8.2	6.63	7.2

Figure 7: Prototyping of RF coupler.

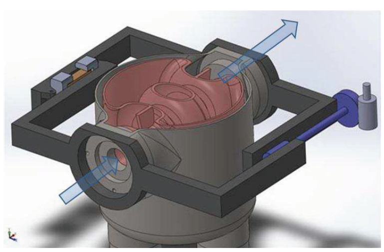

Figure 8: Layout of slow tuner for quarter wave resonator.

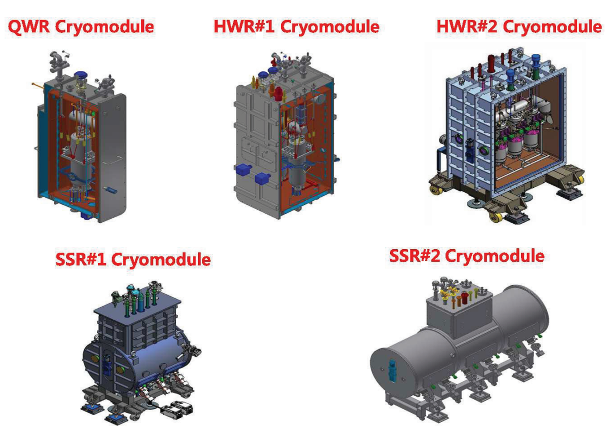

Figure 9: RISP Cryomodules.

Table 4: Thermal Load of Superconducting Linacs

	SCL11	SC12	SCL21	SCL22	SCL31	SCL33
Dynamic (W)	532	2,016	1,014	5,009	532	2,016
Static (W)	227	1,071	475	790	227	1,071
Sum (W)	760	3,087	1,489	5,800	760	3,087

line. High level of vacuum and thermal insulation are required for the cryomodule to maintain the operating temperature of superconducting cavities. The cryomodules including QWR and HWR cavities are box-type while those including SSR1 and SSR2 cavities are cylindrical as shown in Fig. 9. The main components of the cryomodule are dressed cavities and two phase pipe, power couplers to supply RF power to the cavities, tuners to control the operation of the cavities, and support systems to fix the cavities along the beam line. Since the operating temperature of the superconducting cavities are 2 K, 40 K thermal shield and 4.5 K thermal intercepts are installed to minimize the thermal load. The cold mass including cavity string, coupler and tuner is installed on the strong-back and then inserted into the vacuum vessel with thermal shield and MLI. The thermal load of superconducting linacs are summaried in Table 4. Dynamic and static loads are 70% and 30% out of the total thermal load, repectively. The design of the cryomodule components has been conducted based on the thermal and structural concerns. The thermal design starts from the estimation of the thermal loads that determine the required size of the components such as two phase pipes and other cryogenic pipes. Three levels of cryogenic flow are necessary such as 2 K, 4.5 K and 40K.

SUMMARY

The RISP linacs have been presented. In the design, four cavities, such as QWR, HWR, SSR1 and SSR2, are used to accelerate the beam in the linac. The prototype of superconducting cavities have been fabricated and under veritcal test. The box-shaped and cylindrical cryomodules have been designed for hosting cavities and under fabrication.

ACKNOWLEDGMENTS

This work was supported by the Rare Isotope Science Project which is funded by the Ministry of Science, ICT and Future Planning (MSIP) and the National Research Foundation (NRF) of the Republic of Korea under Contract 2011-0032011.

REFERENCES

[1] S.K. Kim et al, "Rare Isotope Science Project: Baseline Design Summary", http://www.risp.re.kr/

[2] H.J. Jang et al, these proc., LINAC 2014, MOPP080

[3] J.-G. Hwang et al, these proc., LINAC 2014, THPP095

[4] H.J. Cha et al, these proc., LINAC 2014, THPP079

[5] M.O. Hyun et al, these proc., LINAC 2014, TUPP083

[6] W.K. Kim et al, these proc., LINAC 2014, TUPP085

ISBN 978-3-95450-142-7